X 5 Berry phase in solid state physics

Ming-Che Chang
Dept. of Physics, National Taiwan Normal Univ.
Taipei, Taiwan

Contents

1 Anholonomy in geometry

Before introducing the Berry phase, we review the elegant mathematical framework behind it. It helps explaining why the Berry phase is often also called the geometric phase.

1.1 Parallel transport and anholonomy angle

Consider a two-dimensional curved surface embedded in a three dimensional Euclidean space. At each point $x = (x_1, x_2)$ on the surface, there is a vector space T_x formed by the tangent vectors at that point. For an ant living on the surface, is it possible to judge if two vectors at different locations (1 and 2) of the surface are nearly parallel or far from it?
One possible way to calibrate the difference between two vectors at different locations is as follows: Starting from point 1, the ant can carry the vector around in such a way that it makes a fixed relative angle with the tangent vector along a path between 1 and 2 (see Fig. 1a). Such a vector is said to be *parallel transported*. One can then compare the vector already at point 2 with the parallel transported vector for difference.
Notice that, if we follow this rule, then "being parallel" is a path-dependent concept. That is, one cannot have a global definition of "being parallel" on the curved surface. The other way to say the same thing is that, if you parallel transport a vector along a closed loop on the surface, then the final vector $\mathbf{v}_f$ is generically different from the initial vector $\mathbf{v}_i$ (see Fig. 1b).
The angle between these two vectors is called the anholonomy angle (or defect angle). Such an angle is an indication of how curved the surface is. One can use it to define the intrinsic curvature of the surface. For example, for a sphere with radius R, the defect angle α for a vector transported around a spherical triangle is equal to the solid angle Ω subtended by this triangle,

$$\alpha = \Omega = \frac{A}{R^2}, \tag{1}$$

where A is the area enclosed by the triangle.
One can define the curvature at point x as the ratio between α and A for an infinitesimally closed loop around x. According to this definition, the sphere has a constant curvature $1/R^2$ everywhere on the surface.
You can apply the same definition to find out the intrinsic curvature of a cylinder. The result would be zero. That is, the cylinder has no intrinsic curvature. That is why we can cut it open and lay it down on top of a desk easily without stretching.

1.2 Moving frame and curvature

In practice, apart from a few simple curved surfaces, it is not easy to determine the curvature without using algebraic tools. At this point, it helps introducing the method of the moving frame. We follow a very nice article by M. Berry (see Berry's introductory article in Ref. [1]) and apply this method to calculate the curvature.
Instead of moving a vector, one now moves an orthonormal frame (a triad) along a path C between two points. At the starting point, the triad is $(\hat{r}, \hat{e}_1, \hat{e}_2)$, where $\hat{r}$ is the unit vector along the normal direction and $(\hat{e}_1, \hat{e}_2)$ is an orthonormal basis of the tangent vector space T_x.
As a rule of parallel transport, we require that, when moving along C, the triad should not twist around $\hat{r}$. That is, if $\boldsymbol{\omega}$ is the angular velocity of the triad, then

$$\boldsymbol{\omega} \cdot \hat{r} = 0. \tag{2}$$

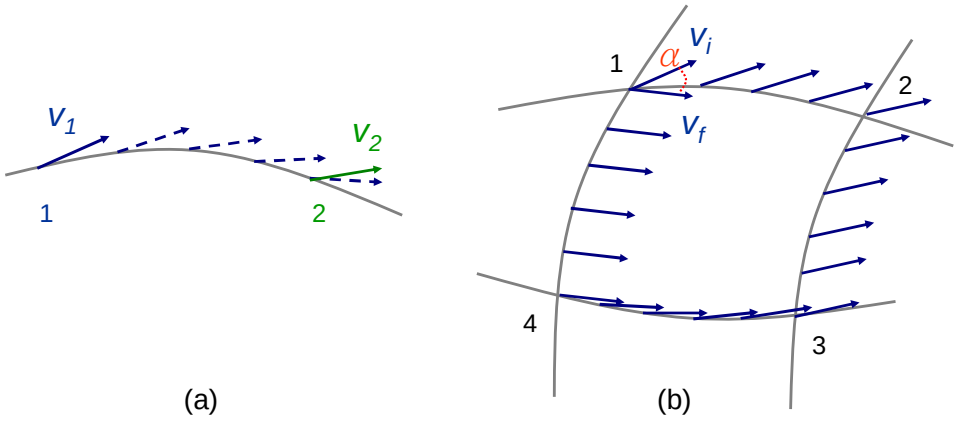

Fig. 1: *(a) Parallel transport of a vector from 1 to 2. It offers a way to compare* $\mathbf{v}_1$ *and* $\mathbf{v}_2$ *on a curved surface. (b) A vector is parallel transported around a closed path. When the surface is curved, the final vector would point to a different direction from the initial vector. The angle of difference* α *is called the anholonomy angle.*

Using the identity $\dot{\hat{e}}_1 = \boldsymbol{\omega} \times \hat{e}_1$ it follows from this requirement that $\dot{\hat{e}}_1 \cdot \hat{e}_2 = 0$:

$$\begin{aligned} \boldsymbol{\omega} \cdot \hat{r} &= \boldsymbol{\omega} \cdot \hat{e}_1 \times \hat{e}_2 \\ &= \boldsymbol{\omega} \times \hat{e}_1 \cdot \hat{e}_2 = \dot{\hat{e}}_1 \cdot \hat{e}_2 = 0. \end{aligned} \tag{3}$$

Likewise also the relation $\dot{\hat{e}}_2 \cdot \hat{e}_1 = 0$ is shown easily.
To make further analogy with the complex quantum phase in the next section, let us introduce the following complex vector,

$$\psi = \frac{1}{\sqrt{2}} \left(\hat{e}_1 + i\hat{e}_2 \right). \tag{4}$$

Then the parallel transport condition can be rephrased as,

$$\mathrm{Im} \left(\psi^* \cdot \dot{\psi} \right) = 0, \text{ or } i\psi^* \cdot \dot{\psi} = 0. \tag{5}$$

Notice that the real part of $\psi^* \cdot \dot{\psi}$ is always zero since $\hat{e}_1 \cdot \hat{e}_1$ and $\hat{e}_2 \cdot \hat{e}_2$ are time independent.
Instead of the moving triad, we could also erect a fixed triad, $(\hat{r}, \hat{u}, \hat{v})$, at each point of the surface and introduce

$$n = \frac{1}{\sqrt{2}} \left(\hat{u} + i\hat{v} \right). \tag{6}$$

Assuming these two triads differ by an angle $\alpha(x)$ (around the $\hat{r}$-axis), then $\psi(x) = n(x)e^{-i\alpha(x)}$. It follows that

$$\psi^* \cdot d\psi = n^* \cdot dn - id\alpha. \tag{7}$$

Because of the parallel transport condition in Eq. (5), one has $d\alpha = -in^* \cdot dn$. Finally, the twist angle accumulated by the moving triad after completing a closed loop C is,

$$\alpha(C) = -i \oint_C n^* \cdot \frac{dn}{dx} dx, \tag{8}$$

where we have changed the variable of integration to the coordinate on the surface. Therefore, the defect angle can be calculated conveniently using the fixed-triad basis.

With the help of the Stokes theorem, one can transform the line integral to a surface integral,

$$\alpha(C) = \int_S \frac{1}{i}\left(\frac{dn^*}{dx_1}\cdot\frac{dn}{dx_2} - \frac{dn^*}{dx_2}\cdot\frac{dn}{dx_1}\right)dx_1dx_2, \tag{9}$$

where S is the area enclosed by C. In the case of the sphere, one can choose (x_1, x_2) to be the spherical coordinates (θ, ϕ), and choose $\hat{u}$ and $\hat{v}$ to be the unit vectors $\hat{\theta}$ and $\hat{\phi}$ in spherical coordinates. That is, $\hat{u} = (\cos\theta\cos\phi, \cos\theta\sin\phi, -\sin\theta)$ and $\hat{v} = (-\sin\phi, \cos\phi, 0)$. It is not difficult to show that the integrand in Eq. (9) is $\sin\theta d\theta d\phi$. Therefore, $\alpha(C)$ is indeed the solid angle of the area S.

The integral in Eq. (9) over the whole sphere (the total curvature) is equal to its solid angle, 4π. In fact, any closed surface that has the same topology as a sphere would have the same total curvature $2\pi \times 2$. The value of 2 (Euler characteristic) can thus be regarded as a number characterizing the topology of sphere-like surfaces. In general, for a closed surface with g holes, the Euler characteristic is $2 - 2g$. For example, the total curvature of a donut ($g = 1$) is 0. This is the beautiful Gauss-Bonnet theorem in differential geometry.

2 Anholonomy in quantum mechanics

Similar to the parallel transported vector on a curved surface, the phase of a quantum state (not including the dynamical phase) may not return to its original value after a cyclic evolution in parameter space. This fact was first exposed clearly by Michael Berry [3] in his 1984 paper. In this section, we introduce the basic concept of the Berry phase, in later sections we will move on to examples of the Berry phase in condensed matter.

2.1 Introducing the Berry phase

Let us start from a time-*independent* system described by a Hamiltonian $H(\mathbf{r}, \mathbf{p})$. We denote the eigenstates by $|m\rangle$ and the eigenvalues by ϵ_m. For simplicity, the energy levels are assumed to be non-degenerate. An initial state $|\psi_0\rangle = \sum a_m|m\rangle$ evolves to a state $|\psi_t\rangle = \sum a_m e^{-i/\hbar\epsilon_m t}|m\rangle$ at time t. The probability of finding a particle in a particular level remains unchanged, even though each level acquires a different dynamical phase $e^{-i/\hbar\epsilon_m t}$. In particular, if one starts with an eigenstate of the Hamiltonian, $|\psi_0\rangle = |n\rangle$, with $a_m = \delta_{m,n}$, then the probability amplitude does not "leak" to other states.

Let us now consider a slightly more complicated system with two sets of dynamical variables $H(\mathbf{r}, \mathbf{p}; \mathbf{R}, \mathbf{P})$. The characteristic time scale of the upper-case set is assumed to be much longer than that of the lower-case set. For example, the system can be a diatomic molecule H_2^+. The electron and nuclei positions are represented by $\mathbf{r}$ and $\mathbf{R}$ respectively. Because of its larger mass, the nuclei move more slowly (roughly by a thousand times) compared to the electron. In the spirit of the Born-Oppenheimer approximation, one can first treat $\mathbf{R}$ as a time-dependent parameter, instead of a dynamical variable, and study the system at each "snapshot" of the evolution. The kinetic part of the slow variable is ignored for now.

Since the characteristic frequency of the nuclei is much smaller than the electron frequency, an electron initially in an electronic state $|n\rangle$ remains essentially in that state after time t,

$$|\psi_t\rangle = e^{i\gamma_n(\mathbf{R})}e^{-i/\hbar\int_0^t dt\epsilon_n(\mathbf{R}_t)}|n;\mathbf{R}\rangle. \tag{10}$$

Table 1: *Anholonomies in geometry and quantum state*

	geometry	quantum state
fixed basis	$n(x)$	$\|n;\mathbf{R}\rangle$
moving basis	$\psi(x)$	$\|\psi;\mathbf{R}\rangle$
parallel-transport condition	$i\psi^*\cdot\dot{\psi}=0$	$i\langle\psi\|\dot{\psi}\rangle=0$
anholonomy	anholonomy angle	Berry phase
classification of topology	Euler characteristic	Chern number

Apart from the dynamical phase, one is allowed to add an extra phase $e^{i\gamma_n(\mathbf{R})}$ for each snapshot state. Such a phase is usually removable by readjusting the phase of the basis $|n;\mathbf{R}\rangle$ [2]. In 1984, almost six decades after the birth of quantum mechanics, Berry [3] pointed out that this phase, like the vector in the previous section, may not return to its original value after a cyclic evolution. Therefore, it is not always removable.

To determine this phase, one substitutes Eq. (10) into the time-*dependent* Schrödinger equation. It is not difficult to get an equation for $\gamma_n(t)$,

$$\dot{\gamma}_n(t)=i\langle n|\dot{n}\rangle. \tag{11}$$

Therefore, after a cyclic evolution, one has

$$\gamma_n(C)=i\oint_C\langle n|\frac{\partial n}{\partial\mathbf{R}}\rangle\cdot d\mathbf{R}=\oint_C\mathbf{A}\cdot d\mathbf{R}, \tag{12}$$

where C is a closed path in the $\mathbf{R}$-space. The integrand $\mathbf{A}(\mathbf{R})\equiv i\langle n|\frac{\partial n}{\partial\mathbf{R}}\rangle$ is often called the *Berry connection*.

If the parameter space is two dimensional, then one can use Stokes' theorem to transform the line integral to a surface integral,

$$\gamma_n(C)=i\int_S\langle\frac{\partial n}{\partial\mathbf{R}}|\times|\frac{\partial n}{\partial\mathbf{R}}\rangle\cdot d^2\mathbf{R}=\int_S\mathbf{F}\cdot d^2\mathbf{R}. \tag{13}$$

The integrand $\mathbf{F}(\mathbf{R})\equiv\nabla_{\mathbf{R}}\times\mathbf{A}(\mathbf{R})$ is usually called the *Berry curvature*. For parameter spaces with higher dimensions, such a transformation can still be done using the language of the differential form.

By now, the analogy between Eqs. (8,9) and Eqs. (12,13) should be clear. Notice that $|n\rangle$ is a normalized basis with $\langle n|n\rangle=1$. Therefore, $\langle n|\dot{n}\rangle$ should be purely imaginary and $i\langle n|\dot{n}\rangle$ is a real number. The basis state $|n\rangle$ plays the role of the fixed triad n in the previous subsection. Both are single-valued. On the other hand, the parallel transported state $|\psi\rangle$ and the moving triad ψ are not single-valued.

A point-by-point re-assignment of the phase of the basis state, $|n;\mathbf{R}\rangle'=e^{ig(\mathbf{R})}|n;\mathbf{R}\rangle$, changes the Berry connection,

$$\mathbf{A}'=\mathbf{A}-\frac{\partial g}{\partial\mathbf{R}}. \tag{14}$$

However, the Berry curvature $\mathbf{F}$ and the Berry phase are not changed. This is similar to the gauge transformation in electromagnetism: one can choose different gauges for the potentials, but the fields are not changed. Such an analogy will be explored further in the next subsection.

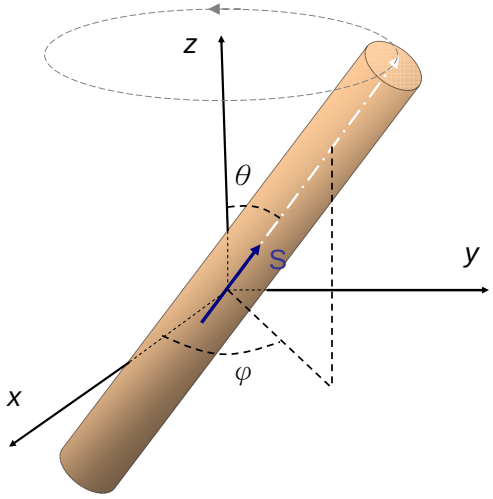

Fig. 2: *A long solenoid hinged at the origin is slowly rotating around the z-axis. At each instant, the spin at the origin aligns with the uniform magnetic field inside the solenoid.*

A short note: It is possible to rephrase the anholonomy of the quantum state using the mathematical theory of fiber bundles, which deals with geometrical spaces that can locally be decomposed into a product space (the "fiber" space times the "base" space), but globally show nontrivial topology. The Möbius band is the simplest example of such a geometric object: Locally it is a product of two one-dimensional spaces but globally it is not (because of the twisting). In our case, the fiber is the space of the quantum phase $\gamma(\mathbf{R})$ and the base is the space of $\mathbf{R}$. The concept of the parallel transport, the connection, and the curvature all can be rephrased rigorously in the language of fiber bundles [4]. Furthermore, there is also a topological number (similar to the Euler characteristic) for the fiber bundle, which is called the Chern number.
The analogy between geometric anholonomy and quantum anholonomy is summarized in Table 1.

2.2 A rotating solenoid

To illustrate the concept of the Berry phase, we study a simple system with both slow and fast degrees of freedom. Following M. Stone [5], we consider a rotating (long) solenoid with an electron spin at its center. The solenoid is tilted with a fixed angle θ and is slowly gyrating around the z-axis (see Fig. 2). Therefore, the electron spin feels a uniform magnetic field that changes direction gradually. This example is a slight generalization of the spin-in-magnetic-field example given by Berry in his 1984 paper. The Hamiltonian of this spin-in-solenoid system is,

$$H = \frac{L^2}{2I} + \mu_B \boldsymbol{\sigma} \cdot \mathbf{B}, \tag{15}$$

where L and I are the angular momentum and the moment of inertia of the solenoid, respectively, and the Bohr magneton is $\mu_B = e\hbar/2mc$.
The magnetic field $\mathbf{B}$ along the direction of the solenoid is our time-dependent parameter $\mathbf{R}$. In the quasi-static limit, the rotation energy of the solenoid is neglected. When the solenoid rotates to the angle (θ, ϕ), the spin eigenstates are

$$|+; \hat{B}\rangle = \begin{pmatrix} \cos\frac{\theta}{2} \\ e^{i\phi}\sin\frac{\theta}{2} \end{pmatrix}, |-; \hat{B}\rangle = \begin{pmatrix} -e^{-i\phi}\sin\frac{\theta}{2} \\ \cos\frac{\theta}{2} \end{pmatrix}. \tag{16}$$

Table 2: *Analogy between electromagnetism and quantum anholonomy*

Electromagnetism	quantum anholonomy
vector potential $\mathbf{A}(\mathbf{r})$	Berry connection $\mathbf{A}(\mathbf{R})$
magnetic field $\mathbf{B}(\mathbf{r})$	Berry curvature $\mathbf{F}(\mathbf{R})$
magnetic monopole	point degeneracy
magnetic flux $\Phi(C)$	Berry phase $\gamma(C)$

These states can be obtained, for example, from the spin-up (-down) states $|\pm\rangle$ by a rotation $e^{-i\boldsymbol{\sigma}\cdot\hat{\theta}(\theta/2)}$, in which the rotation axis $\hat{\theta} = (-\sin\phi, \cos\phi, 0)$ is perpendicular to both $\hat{z}$ and $\hat{B}$. Using the definitions of the Berry connection and the Berry curvature in Eqs. (12) and (13), one obtains

$$\mathbf{A}_{\pm} = \mp\frac{1}{2}\frac{1-\cos\theta}{B\sin\theta}\hat{\phi} \tag{17}$$

$$\mathbf{F}_{\pm} = \mp\frac{1}{2}\frac{\hat{B}}{B^2}. \tag{18}$$

They have the same mathematical structure as the vector potential and the magnetic field of a magnetic monopole. The location of the "monopole" is at the origin of the parameter space, where a point degeneracy occurs. The strength of the monopole $(1/2)$ equals the value of the spin (this is true for larger spins also). That is why the Berry connection and the Berry curvature are sometimes called the Berry potential and the Berry field. In this picture, the Berry phase is equal to the flux of the Berry field passing through a loop C in parameter space. It is easy to see that,

$$\gamma_{\pm}(C) = \mp\frac{1}{2}\Omega(C), \tag{19}$$

where $\Omega(C)$ is the solid angle subtended by loop C with respect to the origin. The similarity between the theory of Berry phase and electromagnetism is summarized in Table 2.

The Berry phase of the fast motion is only half of the story. When the quantum state of the fast variable acquires a Berry phase, there will be an interesting "back action" to the slow motion. For example, for the rotating solenoid, the wave function of the whole system can be expanded as

$$|\Psi\rangle = \sum_{n=\pm}\psi_n(\mathbf{R})|n;\mathbf{R}\rangle, \tag{20}$$

in which $\psi_n(\mathbf{R})$ describes the slow quantum state. From the Schrödinger equation, $H|\Psi\rangle = E|\Psi\rangle$, one can show that,

$$\left[\frac{\hbar^2}{2I\sin^2\theta}\left(\frac{1}{i}\frac{d}{d\phi} - \mathbf{A}_n\right)^2 + \epsilon_n\right]\psi_n = E\psi_n, \tag{21}$$

where ϵ_n is the eigen-energy for the fast degree of freedom, and $\mathbf{A}_n \equiv i\langle n;\mathbf{R}|\frac{d}{d\phi}|n;\mathbf{R}\rangle$. The off-diagonal coupling between $|+\rangle$ and $|-\rangle$ has been ignored. Therefore, the effective Hamiltonian for the slow variable acquires a Berry potential $\mathbf{A}_n(\mathbf{R})$. Such a potential could shift the spectrum and results in a force (proportional to the Berry curvature) upon the slow motion, much like the effect of vector potential $\mathbf{A}(\mathbf{r})$ and magnetic field on a charged particle.

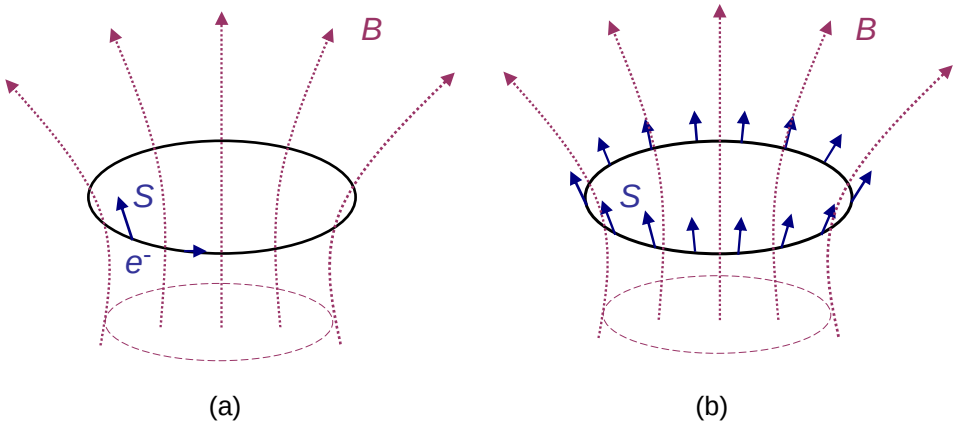

Fig. 3: *(a) A metal ring in a non-uniform magnetic field. The spin of the electron that is circling the ring would align with the magnetic field and trace out a solid angle in its own reference frame. (b) A ferromagnetic ring in a non-uniform magnetic field. The spins on the ring are bent outward because of the magnetic field.*

3 Berry phase and spin systems

A natural place to find the Berry phase is in spin systems. Numerous researches related to this subject can be found in the literature [6]. Here we only mention two examples, one is related to the persistent spin current in a mesoscopic ring, the other relates to quantum tunneling in a magnetic cluster.

3.1 Persistent spin current

We know that an electron moving in a periodic system feels no resistance. The electric resistance is a result of incoherent scatterings from impurities and phonons. If one fabricates a clean one-dimensional wire, wraps it around to form a ring, and lowers the temperature to reduce the phonon scattering, then the electron inside feels like living in a periodic lattice without electric resistance.

For such a design to work, two ingredients are essential: First, the electron has to remain phase coherent (at least partially) after one revolution. Therefore, a mesoscopic ring at very low temperature is usually required. Second, to have a traveling wave, there has to be a phase advance (or lag) after one revolution. This can be achieved by threading a magnetic flux ϕ through the ring, so that the electron acquires an Aharonov-Bohm (AB) phase $(e/\hbar)\phi = 2\pi(\phi/\phi_0)$ after one cycle, where ϕ_0 is the flux quantum h/e. When this does happen, it is possible to observe the resulting *persistent charge current* in the mesoscopic ring.

Soon after this fascinating phenomenon was observed [7], it was proposed that, in addition to the AB phase, a spinful electron can (with proper design) acquire a Berry phase after one cycle, and this can result in a persistent *spin* current [8]. The design is as follows: Instead of a uniform magnetic field, a textured magnetic field is used, so that during one revolution, the electron spin follows the direction of the field and traces out a non-zero solid angle Ω (see Fig. 3a). According to Eq. (19), this gives rise to a spin-dependent Berry phase $\gamma_\sigma(C) = -(\sigma/2)\Omega$, where $\sigma = \pm$. After combining this with the (spin-independent) AB phase, spin-up and spin-down electrons have different phase shifts, generating different amounts of persistent particle current I_+, I_-. Therefore, a spin current defined as $I_s = (\hbar/2)(I_+ - I_-)$ is not zero.

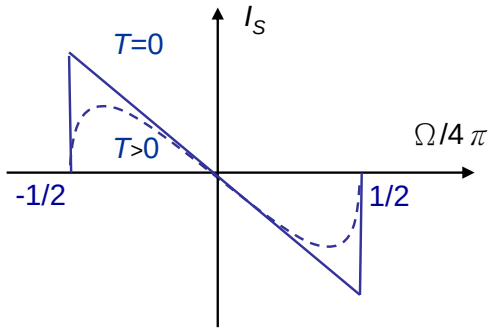

Fig. 4: *Persistent spin current as a function of the solid angle. At non-zero temperature, the sharp edges of the sawtooth become smooth.*

To illustrate the physics just mentioned, consider a ring that allows only angular motion. Before applying the magnetic flux, the electron with wave vector k picks up a phase kL from circling the ring, where $L = 2\pi R$ and R is the radius of the ring. Because of the periodic boundary condition, one has $kL = 2\pi n$ ($n \in Z$). After adding the AB phase and the Berry phase, it becomes $kL = 2\pi n + 2\pi(\phi/\phi_0) - \sigma(\Omega/2)$. Therefore, the energy of an electron in the n-th mode is

$$\epsilon_{n\sigma} = \frac{\hbar^2 k^2}{2m} + \mu_B B\sigma = \frac{\hbar^2}{2mR^2}\left(n + \frac{\phi}{\phi_0} - \sigma\frac{\phi_\Omega}{\phi_0}\right)^2 + \mu_B B\sigma, \tag{22}$$

where $\phi_\Omega/\phi_0 \equiv \Omega/4\pi$.
The spin current can be calculated from

$$I_s = \frac{1}{L}\sum_{n,\sigma}\left(\frac{\hbar}{2}\sigma\right)\frac{\partial\epsilon_{n\sigma}}{\hbar\partial k}P_{n\sigma}, \tag{23}$$

where $P_{n\sigma} = \exp(-\epsilon_{n\sigma}/k_BT)/Z$ is the probability of the electron in the (n,σ)-state, and $Z = \sum_{n,\sigma} e^{-\epsilon_{n\sigma}/k_BT}$. For a particular k and ϕ, the current can also be written as

$$I_s = -\sum_{n,\sigma}\frac{\partial\epsilon_{n\sigma}}{\partial\Omega}P_{n\sigma}. \tag{24}$$

To get a rough understanding, we consider the simplest case, where the $n = 1$ mode is populated with equal numbers of spin-up and -down electrons (if the Zeeman splitting is negligible). The higher modes are all empty at low enough temperature. In this case, the spin current $I_s = -(\hbar^2/4\pi mR^2)(\Omega/4\pi)$ is proportional to the solid angle of the textured magnetic field (see Fig. 4). At higher temperature, the sawtooth curve will become smooth.
The mesoscopic ring considered above is a metal ring with moving electrons that carry the spins with them. A different type of spin current has also been proposed in a ferromagnetic ring with no moving charges [9]. Again the ring is subject to a textured magnetic field, such that when one moves round the ring, one sees a changing spin vector that traces out a solid angle Ω (see Fig. 3b). As a result, the spin wave picks up a Berry phase when traveling around the ring, resulting in a persistent spin current. So far neither type of persistent spin current has been observed experimentally.

3.2 Magnetic cluster

Berry phase plays a dramatic role in the quantum tunneling of nano-sized magnetic clusters. The tunneling between two degenerate spin states of the cluster depends on whether the total spin of the particle is an integer or a half-integer. In the latter case, the tunneling is completely suppressed because different tunneling paths interfere destructively as a result of the Berry phase [10].

Consider a single-domain ferromagnetic particle without itinerant spin. Its total spin J can be of order ten or larger, as long as tunneling is still possible. Assume that the particle lives in an anisotropic environment with the Hamiltonian,

$$H = -k_1 \frac{J_z^2}{J^2} + k_2 \left(\frac{J_x^2}{J^2} - \frac{J_y^2}{J^2} \right), \ (k_1 > k_2). \tag{25}$$

That is, the easy axis is along the z-axis and the easy plane is the yz-plane. The cluster is in the ground state when the spin points to the north pole or to the south pole of the Bloch sphere. Even though these two degenerate states are separated by a barrier, the particle can switch its direction of spin via quantum tunneling.

To study the Berry phase effect on the tunneling probability, the best tool is the method of path integrals. In the following, we give a brief sketch of its formulation.

The fully polarized spin state $|\hat{n}, J\rangle$ along a direction $\hat{n}$ with spherical angles (θ, ϕ) can be written as,

$$\begin{aligned} |\hat{n}, J\rangle &= |\hat{n}, +\rangle \otimes |\hat{n}, +\rangle \cdots \otimes |\hat{n}, +\rangle \\ &= \prod_{l=1}^{2J} e^{-i\frac{\theta}{2}\boldsymbol{\sigma}_l \cdot \hat{\theta}} |\hat{z}, +\rangle_l, \end{aligned} \tag{26}$$

where $|\hat{n}, +\rangle$ is the spin-1/2 "up" state along the $\hat{n}$-axis and $\hat{\theta}$ is a unit vector along the $\hat{z} \times \hat{n}$ direction. Such a so-called *spin coherent state* can be used to "resolve" the identity operator [11],

$$I = \frac{2J+1}{4\pi} \int d\Omega |\hat{n}\rangle\langle\hat{n}|, \tag{27}$$

where $|\hat{n}\rangle$ is an abbreviation of $|\hat{n}, J\rangle$.

In order to calculate the transition probability amplitude $\langle \hat{n}_f | \exp[-(i/\hbar)HT] | \hat{n}_i \rangle$, one first divides the time evolution into steps, $\exp(-i/\hbar HT) = [\exp(-i/\hbar H dt)]^N$, $dt = T/N$, then insert the resolution of identity in Eq. (27) between neighboring steps. The transition amplitude then becomes a product of factors with the following form,

$$\begin{aligned} \langle \hat{n}(t+dt) | e^{-\frac{i}{\hbar}Hdt} | \hat{n}(t) \rangle &\simeq \langle \hat{n}(t+dt) | \hat{n}(t) \rangle - \frac{i}{\hbar} \langle \hat{n}(t+dt) | H(\mathbf{J}) | \hat{n}(t) \rangle dt \\ &\simeq 1 - \langle \hat{n} | \dot{\hat{n}} \rangle dt - \frac{i}{\hbar} H(J\hat{n}) dt. \end{aligned} \tag{28}$$

In the final step, we have replaced the quantum Hamiltonian by a classical Hamiltonian. That is, $\langle H(\mathbf{J}) \rangle = H(\langle \mathbf{J} \rangle)$. This holds exactly if the Hamiltonian is linear in $\mathbf{J}$, but is only an approximation in general. The correction due to the non-commutativity of the spin operator is roughly of the fraction $1/J$ and can be ignored for large spins.

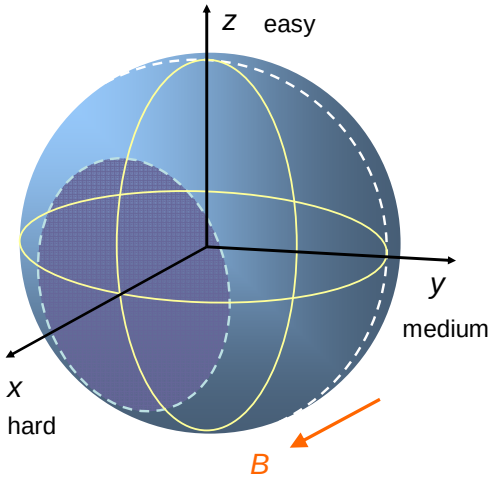

Fig. 5: *According to the Hamiltonian in Eq. (25), the z-axis and the x-axis are the easy axis and the hard axis, respectively. There are two (degenerate) ground states at the north pole and the south pole of the Bloch sphere. Tunneling from one ground state to the other follows the dashed line on the $y-z$ plane. Applying a magnetic field along the x-direction moves the locations of the ground states and shrinks the tunneling path to a smaller loop.*

Finally, by summing over paths in the $\hat{n}$-space, one has

$$\langle \hat{n}_f | e^{-\frac{i}{\hbar}HT} | \hat{n}_i \rangle = \int [\mathcal{D}\hat{n}] \exp\left\{ \frac{i}{\hbar} \int_{t_i}^{t_f} \left[i\hbar \langle \hat{n} | \dot{\hat{n}} \rangle - H(J\hat{n}) \right] dt \right\}. \tag{29}$$

Notice that the first integral in the exponent generates a Berry phase for a path (see Eq. (12)). In the semiclassical regime, the functional integral in Eq. (29) is dominated by the classical path $\hat{n}_c$ with least action, which is determined from the dynamical equation of $\hat{n}$ (see below). During tunneling, the paths under the barrier are classically inaccessible and $\hat{n}$ becomes an imaginary vector. It is customary to sacrifice the reality of time t to keep $\hat{n}$ real. The good news is that the final result does not depend on which imaginary world you choose to live in.
Define $\tau = it$, then the transition amplitude dominated by the classical action is,

$$\langle \hat{n}_f | e^{-\frac{i}{\hbar}HT} | \hat{n}_i \rangle \propto e^{i\int_i^f \mathbf{A}\cdot d\hat{n}_c} e^{-1/\hbar \int_i^f H(J\hat{n}_c) d\tau}, \tag{30}$$

where $\mathbf{A} = i\langle \hat{n} | \nabla \hat{n} \rangle$ is the Berry potential. The integral of the Berry potential is gauge dependent if the path is open. It is well defined for a closed loop, such as the classical path on the yz-plane in Fig. 5. The Berry phase for such a loop is $2\pi J$ since it encloses an area with solid angle 2π (Cf. Eq. (19)). This is also the phase difference between the two classical paths from the north pole to the south pole. Therefore,

$$\langle -\hat{z} | e^{-\frac{i}{\hbar}HT} | \hat{z} \rangle \propto \cos(\pi J) e^{-1/\hbar \int_i^f H(J\hat{n}_c) d\tau}. \tag{31}$$

When J is a half integer, the transition process is completely suppressed because of the Berry phase. The conclusion remains valid if one considers classical paths with higher winding numbers [10].
As a reference, we also write down the equation of motion for $\hat{n}_c$ that is determined from the classical action in Eq. (30),

$$J\frac{d\hat{n}}{dt} = \hat{n} \times \frac{\partial H(J\hat{n})}{\partial \hat{n}}. \tag{32}$$

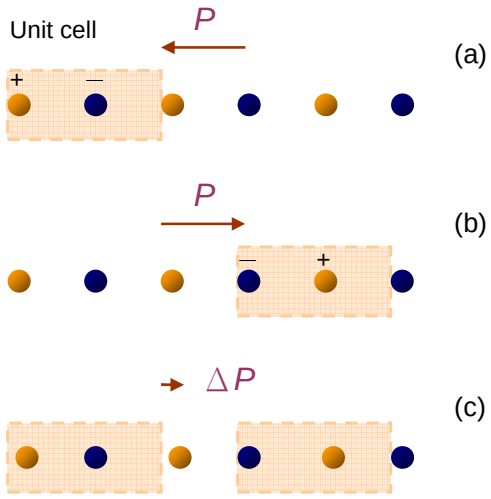

Fig. 6: *An one-dimensional solid with infinite length. Different choices of the unit cell give different electric polarization vectors ((a), (b)). On the other hand, the change of polarization does not depend on the choice of the unit cell (c).*

This is the Bloch equation for spin precession, in which $\partial H/\partial \hat{n}$ plays the role of an effective magnetic field.
One comment is in order: One can apply a magnetic field along the x-axis that shifts the energy minima along that direction and shrinks the classical loop (see Fig. 5). In an increasingly stronger field, the size of the loop C eventually would shrink to zero. That is, the Berry phase γ_C would decrease from the maximum value of $2\pi J$ to zero. During the process, one expects to encounter the no-tunneling situation several times whenever $\gamma_C/2\pi$ hits a half-integer. Such a dramatic Berry phase effect has been observed [12].

4 Berry phase and Bloch state

In the second half of this article, we focus on the Berry phase in *periodic* solids. It has been playing an ever more important role in recent years due to several discoveries and "re-discoveries", in which the Berry phase either plays a crucial role or offers a fresh perspective.

4.1 Electric polarization

It may come as a surprise to some people that the electric polarization $\mathbf{P}$ of an infinite periodic solid (or a solid with periodic boundary conditions) is generically not well defined. The reason is that, in a periodic solid, the electric polarization depends on your choice of the unit cell (see Fig. 6a,b). The theory of electric polarization in conventional textbooks applies only to solids consisting of well localized charges, such as ionic or molecular solids (Clausius-Mossotti theory). It fails, for example, in a covalent solid with bond charges such that no natural unit cell can be defined.
A crucial observation made by R. Resta [13] is that, even though the value of $\mathbf{P}$ may be ambiguous, its change is well defined (see Fig. 6c). It was later pointed out by King-Smith and Vanderbilt [14] that $\Delta\mathbf{P}$ has a deep connection with the Berry phase of the electronic states. The outline of their theory below is based on one-particle states. However, the same scheme

applies to real solids with electronic interactions, as long as one replaces the one-particle states by the Kohn-Sham orbitals in the density functional theory.
We will use λ to label the degree of ion displacement. It varies from 0 to 1 as the ions shift adiabatically from an initial state to a final state. The difference of polarizations between these two states is given by $\int_0^1 d\lambda d\mathbf{P}/d\lambda$, where

$$\mathbf{P}(\lambda) = \frac{q}{V}\sum_i \langle\phi_i|\mathbf{r}|\phi_i\rangle. \tag{33}$$

The summation runs over filled Bloch states ϕ_i (with λ-dependence) and V is the volume of the material. For an infinite crystal, the expectation value of $\mathbf{r}$ is ill-defined. Therefore, we consider a finite system at first, and let $V \to \infty$ when the mathematical expression becomes well-defined.
The Bloch states are solutions of the Schrödinger equation,

$$H_\lambda|\phi_i\rangle = \left(\frac{p^2}{2m} + V_\lambda\right)|\phi_i\rangle = \epsilon_i|\phi_i\rangle, \tag{34}$$

where V_λ is the crystal potential. From Eq. (34), it is not difficult to show that, for $j \neq i$, one has

$$(\epsilon_i - \epsilon_j)\,\langle\phi_j|\frac{\partial\phi_i}{\partial\lambda}\rangle = \langle\phi_j|\frac{\partial V_\lambda}{\partial\lambda}|\phi_i\rangle. \tag{35}$$

Therefore,

$$\frac{d\mathbf{P}}{d\lambda} = \frac{q}{V}\sum_i\sum_{j\neq i}\left[\langle\phi_i|\mathbf{r}|\phi_j\rangle\frac{\langle\phi_j|V'_\lambda|\phi_i\rangle}{\epsilon_i - \epsilon_j} + H.c.\right]. \tag{36}$$

There is a standard procedure to convert the matrix elements of $\mathbf{r}$ to those of $\mathbf{p}$: Start with the commutation relation, $[\mathbf{r}, H_\lambda] = i\hbar\mathbf{p}/m$, and sandwich it between the i-state and the j-state (again $j \neq i$), we can get an useful identity,

$$\langle\phi_i|\mathbf{r}|\phi_j\rangle = \frac{i\hbar}{m}\frac{\langle\phi_i|\mathbf{p}|\phi_j\rangle}{\epsilon_j - \epsilon_i}. \tag{37}$$

With the help of this identity, Eq. (36) becomes the following expression derived by Resta [13],

$$\frac{d\mathbf{P}}{d\lambda} = \frac{q\hbar}{imV}\sum_i\sum_{j\neq i}\left[\frac{\langle\phi_i|\mathbf{p}|\phi_j\rangle\langle\phi_j|V'_\lambda|\phi_i\rangle}{(\epsilon_i - \epsilon_j)^2} - H.c.\right]. \tag{38}$$

Now all of the matrix elements are well-defined and the volume V can be made infinite. After integrating with respect to λ, the resulting $\Delta\mathbf{P}$ is free of ambiguity, even for an infinite covalent solid.
For Bloch states, the subscripts are $i = (m, \mathbf{k})$ and $j = (n, \mathbf{k})$, where m, n are the band indices and $\mathbf{k}$ is the Bloch momentum defined in the first Brillouin zone. Eq. (38) can be transformed to a very elegant form, revealing its connection with the Berry curvature [14]. One first defines a $\mathbf{k}$-dependent Hamiltonian, $\tilde{H} = e^{-i\mathbf{k}\cdot\mathbf{r}}He^{i\mathbf{k}\cdot\mathbf{r}}$. It is the Hamiltonian of the cell-periodic function $u_{n\mathbf{k}}$. That is, $\tilde{H}|u_{n\mathbf{k}}\rangle = \epsilon_{n\mathbf{k}}|u_{n\mathbf{k}}\rangle$, where $\phi_{n\mathbf{k}} = e^{i\mathbf{k}\cdot\mathbf{r}}u_{n\mathbf{k}}$. It is then straightforward to show that,

$$\langle\phi_{m\mathbf{k}}|\mathbf{p}|\phi_{n\mathbf{k}}\rangle = \frac{m}{\hbar}\langle u_{m\mathbf{k}}|\left[\frac{\partial}{\partial\mathbf{k}}, \tilde{H}\right]|u_{n\mathbf{k}}\rangle = \frac{m}{\hbar}(\epsilon_{n\mathbf{k}} - \epsilon_{m\mathbf{k}})\langle u_{m\mathbf{k}}|\frac{\partial u_{n\mathbf{k}}}{\partial\mathbf{k}}\rangle. \tag{39}$$

With the help of this equation and another one very similar to Eq. (35) (just replace the ϕ_i's by the u_i's), we finally get ($\alpha = x, y, z$)

$$\begin{aligned} \frac{dP_\alpha}{d\lambda} &= -\frac{iq}{V}\sum_{n\mathbf{k}}\left(\left\langle\frac{\partial u_{n\mathbf{k}}}{\partial k_\alpha}|\frac{\partial u_{n\mathbf{k}}}{\partial\lambda}\right\rangle - \left\langle\frac{\partial u_{n\mathbf{k}}}{\partial\lambda}|\frac{\partial u_{n\mathbf{k}}}{\partial k_\alpha}\right\rangle\right) \\ &= -\frac{q}{V}\sum_{n\mathbf{k}}\Omega^n_{k_\alpha\lambda}(\mathbf{k}), \end{aligned} \tag{40}$$

where $\Omega^n_{k_\alpha\lambda} \equiv i\left(\langle\frac{\partial u}{\partial k_\alpha}|\frac{\partial u}{\partial\lambda}\rangle - c.c.\right)$ is the Berry curvature for the n-th band in the parameter space of k_α and λ (Cf. Eq. (13)).
Let us take a one-dimensional system as an example. Assuming the lattice constant is a. Then the difference of polarization is ($q = -e$),

$$\Delta P = \frac{e}{2\pi}\sum_n\int_0^{2\pi/a}dk\int_0^1 d\lambda\Omega^n_{k\lambda}. \tag{41}$$

The area of integration is a rectangle with lengths 1 and $2\pi/a$ on each side. The area integral can be converted to a line integral around the boundary of the rectangle, which gives the Berry phase γ_n of such a loop. Therefore,

$$\Delta P = e\sum_n\frac{\gamma_n}{2\pi}. \tag{42}$$

In the special case where the final state of the deformation V_1 is the same as the initial state V_0, the Berry phase γ_n can only be integer multiples of 2π [14]. Therefore, the polarization P for a crystal state is uncertain by an integer charge Q.
One the other hand, this integer charge Q does carry a physical meaning when it is the difference ΔP between two controlled states. For example, when the lattice potential is shifted by one lattice constant to the right, this Q is equivalent to the total charge being transported. Based on such a principle, it is possible to design a quantum charge pump using a time-dependent potential [15].

4.2 Quantum Hall effect

The quantum Hall effect (QHE) has been discovered by K. von Klitzing *et al.* [16] in a two-dimensional electron gas (2DEG) at low temperature and strong magnetic field. Under such conditions, the Hall conductivity σ_H develops plateaus in the $\sigma_H(B)$ plot. For the integer QHE, these plateaus always locate at integer multiples of e^2/h to great precision, irrespective of the samples being used. Such a behavior is reminiscent of macroscopic quantum phenomena, such as the flux quantization in a superconductor ring.
To explain the integer QHE, Laughlin wraps the sheet of the 2DEG to a cylinder to simulate the superconductor ring, and studies the response of the current with respect to a (fictitious) magnetic flux through the cylinder (see Fig. 7). He found that, as the flux increases by one flux quantum h/e, integer charges $Q = ne$ are transported from one edge of the cylinder to the other [17]. This charge transport in the transverse direction gives the Hall current, and the integer n can be identified with the integer of the Hall conductance ne^2/h [18].

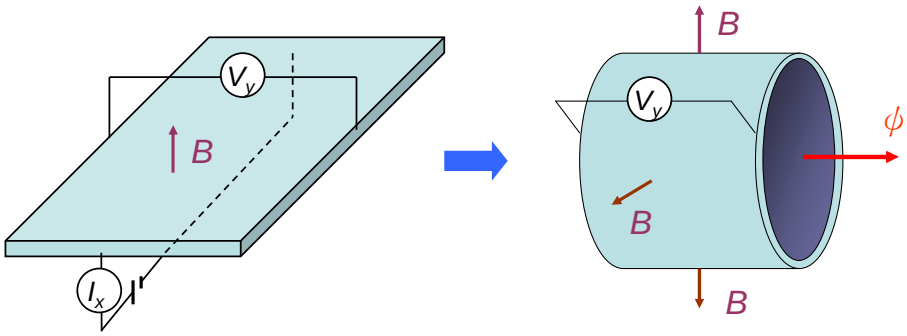

Fig. 7: *In Laughlin's argument, the 2DEG is on the surface of a cylinder. The real magnetic field B now points radially outward. In addition, there is a fictitious flux threading through the cylinder. When the fictitious flux changes by one flux quantum, integer number of electrons are be transported from one edge of the cylinder to the other.*

Soon afterwards, Thouless *et al.* (TKNdN) [19] found that the Hall conductivity is closely related to the Berry curvature (not yet discovered by Berry at that time) of the Bloch state. We now briefly review the TKNdN theory.

Consider a 2DEG subject to a perpendicular magnetic field and a weak in-plane electric field. In order not to break the periodicity of the scalar potential, we choose a time-dependent gauge for the electric field. That is, $\mathbf{E} = -\partial \mathbf{A}_E/\partial t$, $\mathbf{A}_E = -\mathbf{E}t$. The Hamiltonian is,

$$H = \frac{(\boldsymbol{\pi} - e\mathbf{E}t)^2}{2m} + V_L(\mathbf{r}), \tag{43}$$

where $\boldsymbol{\pi} = \mathbf{p} + e\mathbf{A}_0$ has included the vector potential of the magnetic field, and V_L is the lattice potential. Similar to the formulation the in previous subsection, it is convenient to use the k-dependent Hamiltonian $\tilde{H}$ and the cell-periodic function $u_{n\mathbf{k}}$ in our discussion. They are related by $\tilde{H}|u_{n\mathbf{k}}\rangle = E_{n\mathbf{k}}|u_{n\mathbf{k}}\rangle$.

We will assume that the system can be solved with known eigenvalues and eigenstates, $\tilde{H}_0|u^{(0)}_{n\mathbf{k}}\rangle = E^{(0)}_{n\mathbf{k}}|u^{(0)}_{n\mathbf{k}}\rangle$ in the absence of an external electric field [20]. The electric field is then treated as a perturbation. To the first-order perturbation, one has

$$|u_{n\mathbf{k}(t)}\rangle = |n\rangle - i\hbar \sum_{n' \neq n} \frac{|n'\rangle\langle n'|\frac{\partial}{\partial t}|n\rangle}{\epsilon_n - \epsilon_{n'}}, \tag{44}$$

where $\mathbf{k}(t) = \mathbf{k}_0 - e\mathbf{E}t/\hbar$, and $|n\rangle$ and ϵ_n are abbreviations of $|u^{(0)}_{n\mathbf{k}(t)}\rangle$ and $E^{(0)}_{n\mathbf{k}(t)}$.

The velocity of a particle in the n-th band is given by $\mathbf{v}_n(\mathbf{k}) = \langle u_{n\mathbf{k}}|\partial\tilde{H}/\hbar\partial\mathbf{k}|u_{n\mathbf{k}}\rangle$. After substituting the states in Eq. (44), we find

$$\mathbf{v}_n(\mathbf{k}) = \frac{\partial \epsilon_n}{\hbar \partial \mathbf{k}} - i \sum_{n' \neq n} \left(\frac{\langle n|\frac{\partial \tilde{H}}{\partial \mathbf{k}}|n'\rangle\langle n'|\frac{\partial n}{\partial t}\rangle}{\epsilon_n - \epsilon_{n'}} - c.c. \right). \tag{45}$$

The first term is the group velocity in the absence of the electric perturbation. With the help of an equation similar to Eq. (39),

$$\langle n|\frac{\partial \tilde{H}}{\partial \mathbf{k}}|n'\rangle = (\epsilon_n - \epsilon_{n'})\,\langle \frac{\partial n}{\partial \mathbf{k}}|n'\rangle, \tag{46}$$

one finally gets a neat expression,

$$\mathbf{v}_n(\mathbf{k}) = \frac{\partial \epsilon_n}{\hbar \partial \mathbf{k}} - i\left(\left\langle \frac{\partial n}{\partial \mathbf{k}} | \frac{\partial n}{\partial t} \right\rangle - \left\langle \frac{\partial n}{\partial t} | \frac{\partial n}{\partial \mathbf{k}} \right\rangle\right). \tag{47}$$

By a change of variable, the second term becomes $\mathbf{\Omega}_n \times \dot{\mathbf{k}} = -(e/\hbar)\mathbf{\Omega}_n \times \mathbf{E}$, where $\Omega_{n\alpha} = i\epsilon_{\alpha\beta\gamma}\langle \frac{\partial n}{\partial k_\beta} | \frac{\partial n}{\partial k_\gamma} \rangle$ is the Berry curvature in momentum space.
For a 2DEG, $\mathbf{\Omega}_n = \Omega_n \hat{z}$. All states below the Fermi energy contribute to the current density,

$$\mathbf{j} = \frac{1}{V}\sum_{n\mathbf{k}} -e\mathbf{v}_n(\mathbf{k}) = \frac{e^2}{\hbar}\sum_n \int \frac{d^2\mathbf{k}}{(2\pi)^2}\mathbf{\Omega}_n(\mathbf{k}) \times \mathbf{E}. \tag{48}$$

Notice that the first term in Eq. (47) does not contribute to the current. From Eq. (48), it is clear that the Hall conductivity is given by,

$$\sigma_{yx} = \frac{e^2}{h}\sum_n \frac{1}{2\pi}\int d^2\mathbf{k}\Omega_n(\mathbf{k}). \tag{49}$$

Thouless *et al.* have shown that the integral of the Berry curvature over the whole BZ divided by 2π must be an integer c_n. Such an integer (the Chern number mentioned in Sec. 2.2) characterizes the topological property of the fiber bundle space, in which the base space is the two-dimensional BZ, and the fiber is the phase of the Bloch state (see the discussion near the end of Sec. 2.1). Therefore, the Hall conductivity of a filled band is always an integer multiple of e^2/h. Such a topological property is the reason why the QHE is so robust against disorders and sample varieties. Even though the discussion here is based on single-particle Bloch states, the conclusion remains valid for many-body states [21].
Some comments are in order. First, the formulas behind the change of electric polarization $\Delta\mathbf{P}$ in Sec. 4.1 and those of the quantum Hall conductivity here look very similar. Both are based on the linear response theory. In fact, the analogy can be carried further if $\Delta\mathbf{P}$ is considered as the time integral of a polarization current $\mathbf{j}_P = \partial\mathbf{P}/\partial t$. The latter, similar to the quantum Hall current in Eq. (48), can be related to the Berry curvature directly.
Second, if a solid is invariant under space inversion, then the cell-periodic state has the symmetry,

$$u_{n-\mathbf{k}}(-\mathbf{r}) = u_{n\mathbf{k}}(\mathbf{r}). \tag{50}$$

On the other hand, if the system has time-reversal symmetry, then

$$u^*_{n-\mathbf{k}}(\mathbf{r}) = u_{n\mathbf{k}}(\mathbf{r}). \tag{51}$$

As a result, if both symmetries exist, then one can show that the Berry potential $\mathbf{A}_n = i\langle n|\frac{\partial n}{\partial \mathbf{k}}\rangle$ (and therefore the Berry curvature) is zero for all $\mathbf{k}$. The conclusion, however, does not hold if there is band crossing or spin-orbit interaction (not considered so far).
That is, the Berry potential (or curvature) can be non-zero if (i) the lattice does not have space inversion symmetry. This applies to the polarization discussed in the previous subsection. (ii) Time-reversal symmetry is broken, e.g., by a magnetic field. This applies to the quantum Hall system in this subsection. In the next subsection, we consider a system with spin-orbit interaction, in which the Berry curvature plays an important role.

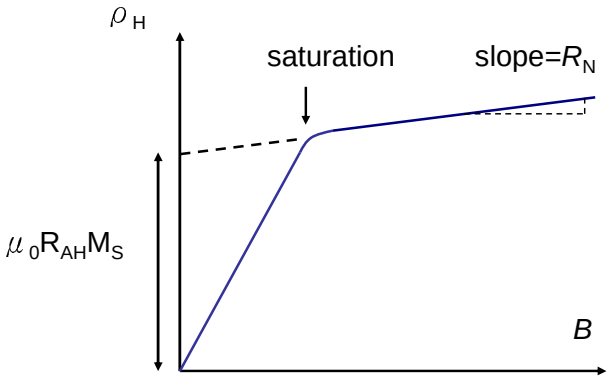

Fig. 8: *When one increases the magnetic field, the Hall resistivity of a ferromagnetic material rises quickly. It levels off after the sample is fully magnetized.*

4.3 Anomalous Hall effect

Soon after Edwin Hall discovered the effect that bears his name in 1879 (at that time he was a graduate student at Johns Hopkins university), he made a similar measurement on iron foil and found a much larger Hall effect. Such a Hall effect in ferromagnetic materials is called the anomalous Hall effect (AHE).

The Hall resistivity of the AHE can be divided into two terms with very different physics (proposed by Smith and Sears in 1929) [22],

$$\rho_H = \rho_N + \rho_{AH} = R_N(T)B + R_{AH}(T)\mu_0 M(T,H), \tag{52}$$

where $B = \mu_0(H + M)$. The first (normal) term is proportional to the magnetic field in the sample. The second (anomalous) term grows roughly linearly with the magnetization M and the coefficient R_{AH} is larger than R_N by one order of magnitude or more. If the applied field is so strong that the material is fully magnetized, then there is no more enhancement from the anomalous term and the Hall coefficient suddenly drops by orders of magnitude (see Fig. 8). Since the normal term is usually much smaller than the anomalous term, we will neglect it in the following discussion.

Unlike the ordinary Hall effect, the Hall *resistivity* in the AHE increases rapidly with temperature. However, the Hall *conductivity*,

$$\sigma_H = \frac{\rho_H}{\rho_L^2 + \rho_H^2} \simeq \frac{\rho_H}{\rho_L^2} \quad (\text{if } \rho_L \gg \rho_H), \tag{53}$$

shows less temperature dependence, where ρ_L is the longitudinal resistivity. The reason will become clear later.

Since the AHE is observed in ferromagnetic materials, the magnetization (or the majority spin) must play a role here. Also, one needs the spin-orbit (SO) interaction to convert the direction of the magnetization to a preferred direction of the transverse electron motion.

Among many attempts to explain the AHE, there are two popular explanations [23], both involve the SO interaction,

$$H_{SO} = -\frac{\hbar}{4m^2c^2}\boldsymbol{\sigma} \cdot (\mathbf{p} \times \nabla V). \tag{54}$$

The first theory was proposed by Karplus and Luttinger (KL) in 1954 [24]. It requires no impurity (the intrinsic scenario) and the V in Eq. (54) is the lattice potential. The Hall resistivity

ρ_{AH} is found to be proportional to ρ_L^2. The other explanation is proposed by Smit in 1958 [25]. It requires (non-magnetic) impurities (the extrinsic scenario) and V is the impurity potential. It predicts $\rho_{AH} \propto \rho_L$. When both mechanisms exist, one has

$$\rho_{AH} = a(M)\rho_L + b(M)\rho_L^2. \tag{55}$$

The Smit term is a result of the skewness of the electron-impurity scattering due to the SO interaction. That is, the spin-up electrons prefer scattering to one side, and the spin-down electrons to the opposite side. Because of the majority spins of the ferromagnetic state, such skew-scatterings produce a net transverse current. Smit's proposal started as an opposition to KL's theory and gained popularity in the early years. As a result, the KL scenario seems to have been ignored for decades.

At the turn of this century, however, several theorists picked up the KL theory and put it under the new light of the Berry curvature [26]. Subsequently, increasing experimental evidences indicate that, in several ferromagnetic materials, the KL mechanism does play a much more important role than the skew-scattering. These works published in renowned journals have attracted much attention, partly because of the beauty of the Berry curvature scenario.

KL's theory, in essence, is very similar to the ones in the previous two subsections. One can first regard the Hamiltonian with the SO interaction as solvable, then treat the electric field as a perturbation. To the first order of the perturbation, one can get the electron velocity with exactly the same form as the one in Eq. (47). The difference is that the state $|n\rangle$ now is modified by the SO interaction and the solid is three dimensional. That is, one simply needs to consider a periodic solid without impurities and apply the Kubo formula, which (in these cases) can be written in Berry curvatures,

$$\sigma_{AH} = \frac{e^2}{\hbar}\frac{1}{V}\sum_{n,\mathbf{k}}\Omega_n(\mathbf{k}). \tag{56}$$

However, not every solid with the SO interaction has the AHE. The transverse velocities (also called the anomalous velocity) in general have opposite signs for opposite spins in the spin-degenerate bands. Therefore, these two Hall currents will get canceled. Again the ferromagnetic state (which spontaneously breaks the time reversal symmetry) is crucial for a net transverse current.

From Eq. (53), one has $\rho_H \simeq \rho_{AH} = \sigma_H \rho_L^2$. Also, the anomalous current generated from the Berry curvature is independent of the relaxation time τ. This explains why the Hall conductivity in the KL theory is proportional to ρ_L^2.

In dilute magnetic semiconductors, one can show that $\mathbf{A}(\mathbf{k}) = \xi\mathbf{S} \times \mathbf{k}$ for the conduction band of the host semiconductor, where ξ is the strength of the SO coupling (more details in Sec. 5.2). Therefore, $\mathbf{\Omega} = \nabla \times \mathbf{A} = 2\xi\mathbf{S}$. In this case, the coefficient $b(M)$ in Eq. (55) is proportional to M. In ferromagnetic materials with a more complex band structure, the Berry curvature shows non-monotonic behavior in magnetization. For one thing, in density-functional-theory calculations, the Berry curvature can be dramatically enhanced when the Fermi energy is near a small energy gap [27]. However, spin fluctuations may smear out the erratic behavior and lead to a smooth variation (see Fig. 9) [28].

The Berry curvature is an intrinsic property of the electronic states. It appears not only at the quantum level, but also in the semiclassical theory of electron dynamics. In the next section, we will see that the QHE, the AHE, and the spin Hall effect can all be unified in the same semiclassical theory.

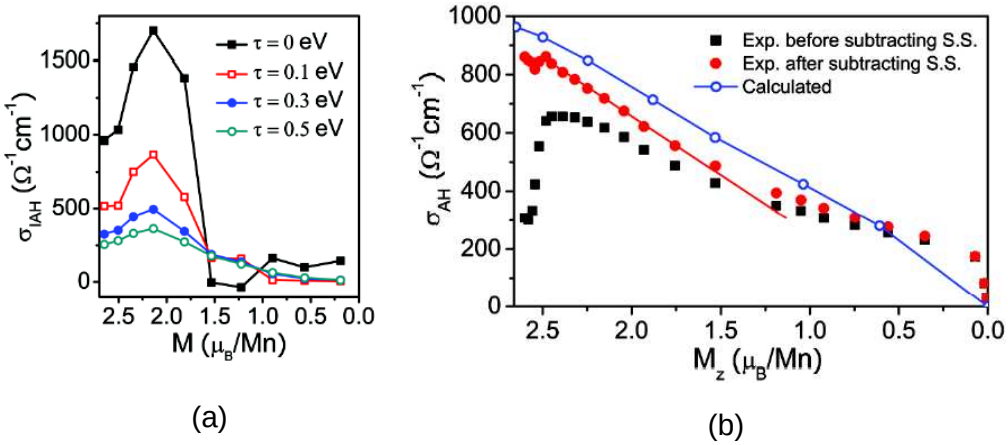

Fig. 9: *(a) Calculated anomalous Hall conductivity (the intrinsic part) versus magnetization for* $\mathrm{Mn_5Ge_3}$ *using different relaxation times. (b) After averaging over long-wavelength spin fluctuations, the calculated anomalous Hall conductivity becomes roughly linear in* M*. The initials S.S. refers to skew scattering. The figures are from Ref. [28].*

5 Berry phase and wave-packet dynamics

When talking about electron transport in solids, people use two different languages: It is either particle scattering, mean free path, cyclotron orbit ..., or localized state, mobility edge, Landau level ... etc. In this section, we use the first language and treat the electrons as particles with trajectories. Besides being intuitive, this approach has the following advantage: The electromagnetic potentials in the Schrödinger equation are often linear in $\mathbf{r}$ and diverge with system size. Such a divergence can be avoided if the wave function of the electron is localized.

5.1 Wave-packet dynamics

Consider an energy band that is isolated from the other bands by finite gaps. Also, the energy band is not degenerate with respect to spin or quasi-spin. The energy band with internal (e.g., spin) degrees of freedom is the subject of the next subsection. When inter-band tunneling can be neglected, the electron dynamics in this energy band can be described very well using a wave-packet formalism.

The wave packet can be built by a superposition of Bloch states $\psi_{n\mathbf{q}}$ in band n (one band approximation),

$$|W\rangle = \int_{BZ} d^3q a(\mathbf{q},t)|\psi_{n\mathbf{q}}\rangle. \tag{57}$$

It is not only localized in position space, but also in momentum space,

$$\langle W|\mathbf{r}|W\rangle = \mathbf{r}_c; \quad \int_{BZ} d^3q \mathbf{q}|a(\mathbf{q})|^2 = \mathbf{q}_c, \tag{58}$$

where $\mathbf{r}_c$ and $\mathbf{q}_c$ are the centers of mass. The shape of the wave packet is not crucial, as long as the electromagnetic field applied is nearly uniform throughout the wave packet.

Instead of solving the Schrödinger equation, we use the time-dependent variational principle to study the dynamics of the wave packet. Recall that in the usual (time-independent) variational principle, one first proposes a sensible wave function with unknown parameters, then minimizes

its energy to determine these parameters. Here, the wave packet is parametrized by its center of mass $(\mathbf{r}_c(t), \mathbf{q}_c(t))$. Therefore, instead of minimizing the energy, one needs to extremize the action $S[C] = \int_C dtL$, which is a *functional* of the trajectory C in phase space.
One starts from the following effective Langrangian,

$$L(\mathbf{r}_c, \mathbf{q}_c; \dot{\mathbf{r}}_c, \dot{\mathbf{q}}_c) = i\hbar\langle W|\frac{d}{dt}|W\rangle - \langle W|H|W\rangle. \tag{59}$$

Notice the resemblance between this $S[C]$ and the the action in the coherent-state path integral (Eq. (29)). The Hamiltonian for a Bloch electron in an electromagnetic field is

$$H = \frac{1}{2m}(\mathbf{p} + e\mathbf{A})^2 + V_L(\mathbf{r}) - e\phi(\mathbf{r}) \simeq H_0 - e\phi + \frac{e}{2m}\mathbf{r} \times \mathbf{p} \cdot \mathbf{B}, \tag{60}$$

in which $H_0 = p^2/2m + V_L$ and ϕ and $\mathbf{A} = \frac{1}{2}\mathbf{B} \times \mathbf{r}$ are treated as perturbations. The fields are allowed to change slowly in space and time, as long as it is approximately uniform and quasi-static (adiabatic) from the wave packet's perspective.
To evaluate the Lagrangian approximately, one can Taylor-expand the potentials with respect to the center of the wave packet and keep only the linear terms. Using this gradient approximation, the wave-packet energy $\langle W|H|W\rangle$ is evaluated as [29],

$$E = E_0(\mathbf{q}_c) - e\phi(\mathbf{r}_c) + \frac{e}{2m}\mathbf{L}(\mathbf{q}_c) \cdot \mathbf{B}, \tag{61}$$

where E_0 is the unperturbed Bloch energy of the band under consideration, and $\mathbf{L}(\mathbf{k}_c) = \langle W|(\mathbf{r} - \mathbf{r}_c) \times \mathbf{p}|W\rangle$ is the self-rotating angular momentum of the wave packet.
On the other hand, the first term in Eq. (59) can be written as

$$i\hbar\langle W|\frac{d}{dt}|W\rangle = \hbar\langle u|i\frac{du}{dt}\rangle + \hbar\mathbf{q}_c \cdot \dot{\mathbf{r}}_c, \tag{62}$$

in which $|u\rangle$ is the unperturbed cell-periodic function. Therefore, the effective Lagrangian is

$$L = \hbar\dot{\mathbf{k}}_c \cdot \mathbf{R}_c + (\hbar\mathbf{k}_c - e\mathbf{A}_c) \cdot \dot{\mathbf{r}}_c - E(\mathbf{r}_c, \mathbf{k}_c), \tag{63}$$

where $\hbar\mathbf{k}_c = \hbar\mathbf{q}_c + e\mathbf{A}_c$ is the gauge-invariant quasi-momentum, $\mathbf{R}_c = i\langle n|\frac{\partial n}{\partial \mathbf{k}_c}\rangle$ is the Berry potential, and $\mathbf{A}_c = \mathbf{A}(\mathbf{r}_c)$.
Treating both $\mathbf{r}_c$ and $\mathbf{k}_c$ as generalized coordinates and using the Euler-Lagrange equation, it is not very difficult to get the following (coupled) equations of motion (EOM) for the wave packet [29],

$$\hbar\dot{\mathbf{k}}_c = -e\mathbf{E} - e\dot{\mathbf{r}}_c \times \mathbf{B}, \tag{64}$$

$$\hbar\dot{\mathbf{r}}_c = \frac{\partial E}{\partial \mathbf{k}_c} - \hbar\dot{\mathbf{k}}_c \times \mathbf{\Omega}_c, \tag{65}$$

where $\mathbf{\Omega}_c = \nabla_{\mathbf{k}_c} \times \mathbf{R}_c$ is the Berry curvature of the band under consideration.
Compared to the usual semiclassical EOM in textbooks, there are two new quantities in Eqs. (64,65), and both lead to important consequences. The first is the Berry curvature $\mathbf{\Omega}$. It generates the so-called anomalous velocity. In the presence of a perturbing electric field, the anomalous velocity is $e\mathbf{E} \times \mathbf{\Omega}$, which is perpendicular to the driving electric field and gives rise to, e.g., the AHE.

The second is the spinning angular momentum $\mathbf{L}$ in Eq. (61). It is closely related to the orbital magnetization of a solid [30]. For a spinful wave packet (Sec. 5.2), this $\mathbf{L}$ modifies the electron spin and is the origin of the anomalous g-factor in solids. In fact, starting from Dirac's relativistic electron theory (which has no explicit spin in the Hamiltonian), we have shown that, the wave packet in the positive-energy branch of the Dirac spectrum has an intrinsic spinning angular momentum [31]. That is, it explains why an electron has spin.
In the semiclassical theory of electron transport, the current density is given by

$$\mathbf{j} = -\frac{e}{V}\sum_{n\mathbf{k}} f\dot{\mathbf{r}}, \tag{66}$$

where $f = f_0 + \delta f$ is the distribution function away from equilibrium. The distribution function f is determined from the Boltzmann equation,

$$\dot{\mathbf{r}}\cdot\frac{\partial f}{\partial \mathbf{r}} + \dot{\mathbf{k}}\cdot\frac{\partial f}{\partial \mathbf{k}} = -\frac{\delta f}{\tau}, \tag{67}$$

where τ is the relaxation time. For a homogeneous system in an electric field, $\delta f \simeq \tau\frac{e}{\hbar}\mathbf{E}\cdot\frac{\partial f_0}{\partial \mathbf{k}}$, and

$$\mathbf{j} \simeq -\frac{e}{V}\sum_{n\mathbf{k}}\left(\delta f\frac{\partial E_n}{\hbar\partial\mathbf{k}} + f_0\frac{e}{\hbar}\mathbf{E}\times\mathbf{\Omega}_n\right). \tag{68}$$

The usual current (the first term) depends on carrier relaxation time τ through the change of the distribution function δf. On the other hand, the second term gives the Hall current. Clearly, this $\mathbf{\Omega}$ is also the one in the Kubo formula of QHE and AHE. (The latter involves spin-degenerate band and belongs more properly to the next subsection.)
We emphasize that, just like the Bloch energy $E_0(\mathbf{k})$, both $\mathbf{\Omega}(\mathbf{k})$ and $\mathbf{L}(\mathbf{k})$ are intrinsic to the energy band (not induced by the applied field). They are the three main pillars of band theory. Unlike the Bloch energy that has been around for a very long time, the other two quantities are relatively new players, but their importance should increase over time.
If there is only a magnetic field, then combining Eq. (64) and Eq. (65) gives

$$\hbar\dot{\mathbf{k}}_c = \frac{-\frac{e}{\hbar}\frac{\partial E}{\partial \mathbf{k}_c}\times\mathbf{B}}{1+\frac{e}{\hbar}\mathbf{B}\cdot\mathbf{\Omega}}. \tag{69}$$

It describes a cyclotron orbit moving on a plane perpendicular to the magnetic field. The orbit is an energy contour on the Fermi surface. Its size can change continuously, depending on the electron's initial condition.
One can apply a Bohr-Sommerfeld quantization rule to get quantized orbits, which have discrete energies (the Landau levels). The EOM in momentum space, Eq. (69), follows from the effective Lagrangian,

$$L(\mathbf{k}_c;\dot{\mathbf{k}}_c) = \frac{\hbar^2}{2eB}\mathbf{k}_c\times\dot{\mathbf{k}}_c\cdot\hat{B} + \hbar\dot{\mathbf{k}}_c\cdot\mathbf{R}_c - E(\mathbf{k}_c). \tag{70}$$

This gives the generalized momentum,

$$\boldsymbol{\pi} = \frac{\partial L}{\partial\dot{\mathbf{k}}_c} = -\frac{\hbar^2}{2eB}\mathbf{k}_c\times\hat{B} + \hbar\mathbf{R}_c. \tag{71}$$

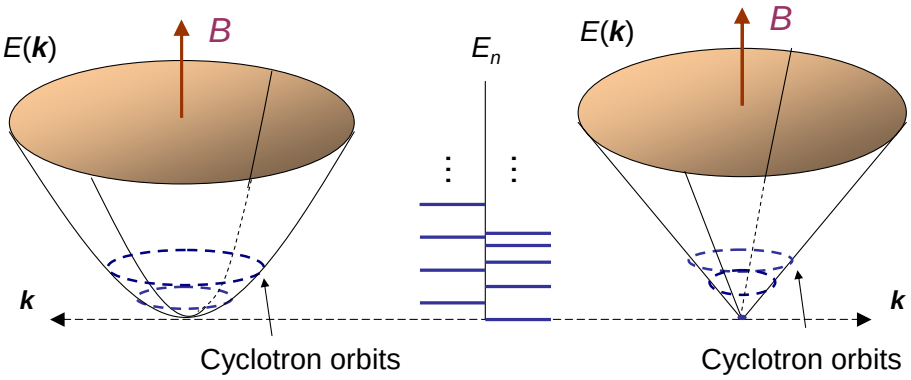

Fig. 10: *The quantized cyclotron orbits on two different energy surfaces. The one on the left is a paraboloid near its band edge; the one on the right is a conical surface. Without Berry phase correction, the Landau-level energies are* $E_n = (n+1/2)\hbar\omega_c$ *and* $E_n = v_F\sqrt{2eB\hbar(n+1/2)}$ *respectively. In graphene, an orbit circling the Dirac point acquires a Berry phase of* π*, which cancels the 1/2 in the square root.*

The quantization condition is given by $\oint \boldsymbol{\pi}\cdot d\mathbf{k}_c = (m+\gamma)h$, where m is a non-negative integer and $\gamma = 1/2$ for the cyclotron motion. Therefore, we have

$$\frac{\hat{B}}{2}\cdot\oint_{C_m}(\mathbf{k}_c\times d\mathbf{k}_c) = 2\pi\left(m+\frac{1}{2}-\frac{\Gamma(C_m)}{2\pi}\right)\frac{eB}{\hbar}, \tag{72}$$

where $\Gamma(C_m) = \oint_{C_m}\mathbf{R}_c\cdot d\mathbf{k}_c$ is the Berry phase for orbit C_m.
This equation determines the allowed size (and therefore energy) of the cyclotron orbit. The Berry phase correction slightly shifts the Landau-level energies. For example, the orbit around the Dirac point of graphene picks up a Berry phase of π due to the monopole at the origin. This cancels the other $1/2$ in Eq. (72) and results in a zero-energy level at the Dirac point (see Fig. 10). This agrees nicely with experimental measurements [32].

5.2 Non-Abelian generalization

In the one-band theory without internal degrees of freedom, the Bloch state has only one component and the gauge structure of the Berry phase is Abelian. When the band has internal degrees of freedom (henceforth simply called the spin), the Bloch state has several components and the gauge structure becomes non-Abelian. This happens, for example, in energy bands with Kramer's degeneracy. By extending the semiclassical dynamics to such cases, one is able to investigate problems involving spin dynamics and spin transport.
The scheme for building such a theory is the same as the one in the previous subsection. Therefore, we only give a very brief outline below. One first constructs a wave packet from the Bloch states $\psi_{n\mathbf{q}}$,

$$|W\rangle = \sum_{n=1}^{D}\int_{BZ} d^3q\, a(\mathbf{q},t)\eta_n(\mathbf{q},t)|\psi_{n\mathbf{q}}\rangle. \tag{73}$$

Here n is a spinor index for an isolated band with D-fold degeneracy, $\boldsymbol{\eta} = (\eta_1,\cdots,\eta_D)^T$ is a normalized spinor at each $\mathbf{q}$, and $a(\mathbf{q},t)$ is again a narrow distribution centered at $\mathbf{q}_c(t)$.
Similar to the non-degenerate case, there are three basic quantities in such a formalism, the Bloch energy $\mathcal{H}_0(\mathbf{q})$, the Berry connection $\boldsymbol{\mathcal{R}}(\mathbf{q})$ (and related curvature, now written as $\boldsymbol{\mathcal{F}}(\mathbf{q})$),

and the spinning angular momentum $\boldsymbol{\mathcal{L}}(\mathbf{q})$ [33]. They all become matrix-valued functions and are denoted by calligraphic fonts. The Bloch energy is simply an identity matrix multiplied by $E_0(\mathbf{q})$ since all spinor states have the same energy.
The matrix elements of the Berry connection are,

$$\mathbf{R}_{mn}(\mathbf{q}) = i\left\langle u_{m\mathbf{q}}|\frac{\partial u_{n\mathbf{q}}}{\partial \mathbf{q}}\right\rangle. \tag{74}$$

The Berry curvature is given by,

$$\boldsymbol{\mathcal{F}}(\mathbf{q}) = \nabla_{\mathbf{q}} \times \boldsymbol{\mathcal{R}} - i\boldsymbol{\mathcal{R}} \times \boldsymbol{\mathcal{R}}. \tag{75}$$

Recall that the Berry connection and Berry curvature in the Abelian case are analogous to the vector potential and the magnetic field in electromagnetism (see Sec. 2.1). Here, $\boldsymbol{\mathcal{R}}$ and $\boldsymbol{\mathcal{F}}$ also are analogous to the gauge potential and gauge field in the non-Abelian $SU(2)$ gauge field theory [34].
The expectation value of the third basic quantity, the spinning angular momentum, is again given by $\mathbf{L}(\mathbf{q}_c) = \langle W|(\mathbf{r}-\mathbf{r}_c)\times\mathbf{p}|W\rangle$. However, it is often written in an alternative (Rammal-Wilkinson) form easier for evaluation,

$$\mathbf{L}(\mathbf{q}) = i\frac{m}{\hbar}\left\langle \frac{\partial u}{\partial \mathbf{q}}\Big|\times\Big[\tilde{H}_0 - E_0(\mathbf{q})\Big]\Big|\frac{\partial u}{\partial \mathbf{q}}\right\rangle, \tag{76}$$

where the cell-periodic function without a subscript is defined as $|u\rangle = \sum_{n=1}^{D}\eta_n|u_n\rangle$ and $\tilde{H}_0$ is the Hamiltonian for $|u\rangle$. The corresponding matrix-valued function $\boldsymbol{\mathcal{L}}$ therefore has the matrix elements,

$$\mathbf{L}_{nl}(\mathbf{q}) = i\frac{m}{\hbar}\left\langle \frac{\partial u_n}{\partial \mathbf{q}}\Big|\times\Big[\tilde{H}_0 - E_0(\mathbf{q})\Big]\Big|\frac{\partial u_l}{\partial \mathbf{q}}\right\rangle. \tag{77}$$

Obviously, after taking the spinor average, one has the angular momentum in Eq. (76), $\mathbf{L} = \langle\boldsymbol{\mathcal{L}}\rangle \equiv \boldsymbol{\eta}^\dagger\boldsymbol{\mathcal{L}}\boldsymbol{\eta} = \sum_{nl}\eta_n^*\mathbf{L}_{nl}\eta_l$.

Equations of motion
So far we have laid out the necessary ingredients in the non-Abelian wave packet theory. Similar to Sec. 5.2, we can use Eq. (59) to get the effective Lagrangian for the center of mass, $(\mathbf{r}_c, \mathbf{k}_c)$, and the spinor $\boldsymbol{\eta}$. Afterwards, the Euler-Lagrange equation for this effective Lagrangian leads to the following EOM [33],

$$\hbar\dot{\mathbf{k}}_c = -e\mathbf{E} - e\dot{\mathbf{r}}_c\times\mathbf{B}, \tag{78}$$

$$\hbar\dot{\mathbf{r}}_c = \left\langle\left[\frac{\mathcal{D}}{\mathcal{D}\mathbf{k}_c},\mathcal{H}\right]\right\rangle - \hbar\dot{\mathbf{k}}_c\times\mathbf{F}, \tag{79}$$

$$i\hbar\dot{\boldsymbol{\eta}} = \left(\frac{e}{2m}\boldsymbol{\mathcal{L}}\cdot\mathbf{B} - \hbar\dot{\mathbf{k}}_c\cdot\boldsymbol{\mathcal{R}}\right)\boldsymbol{\eta}, \tag{80}$$

where $\mathbf{F} = \langle\boldsymbol{\mathcal{F}}\rangle$, and the covariant derivative $\mathcal{D}/\mathcal{D}\mathbf{k}_c \equiv \partial/\partial\mathbf{k}_c - i\boldsymbol{\mathcal{R}}$. The semiclassical Hamiltonian inside the commutator in Eq. (79) is

$$\mathcal{H}(\mathbf{r}_c,\mathbf{k}_c) = \mathcal{H}_0(\mathbf{k}_c) - e\phi(\mathbf{r}_c) + \frac{e}{2m}\boldsymbol{\mathcal{L}}(\mathbf{k_c})\cdot\mathbf{B}, \tag{81}$$

where $\mathbf{k}_c = \mathbf{q}_c + (e/\hbar)\mathbf{A}(\mathbf{r}_c)$.

Even though these equations look a little complicated, the physics is very similar to that of the simpler Abelian case in Sec. 5.1. There are two differences, however. First, the anomalous velocity in Eq. (79) is now spin-dependent in general. In some interesting cases (see below), $\mathbf{F}$ is proportional to the spin vector $\mathbf{S} = \langle \boldsymbol{\mathcal{S}} \rangle$, where $\boldsymbol{\mathcal{S}}$ is the spin matrix. Therefore, if one applies an electric field to such a system, the spin-up and spin-down electrons will move to opposite transverse directions. This is the cause of the AHE and the spin Hall effect.
Second, we now have an additional equation (Eq. (80)) governing the spinor dynamics. From Eq. (80) we can derive the equation for $\mathbf{S}$,

$$i\hbar\dot{\mathbf{S}} = \left\langle \left[\boldsymbol{\mathcal{S}}, \mathcal{H} - \hbar\dot{\mathbf{k}}_c \cdot \boldsymbol{\mathcal{R}} \right] \right\rangle . \tag{82}$$

The spin dynamics in Eq. (82) is influenced by the Zeeman energy in $\mathcal{H}$, as it should be. We will demonstrate below that the term with the Berry connection is in fact the spin-orbit energy. Such an energy is not explicit in $\mathcal{H}$, but only reveals itself after $\mathcal{H}$ is being re-quantized.

Re-quantization
As we have shown in Sec. 5.1, re-quantization of the semiclassical theory is necessary when one is interested in, for example, the quantized cyclotron orbits that correspond to the Landau levels. Here we introduce the method of canonical quantization, which is more appropriate for the non-Abelian case compared to the Bohr-Sommerfeld method.
In this approach, one needs to find variables with canonical Poisson brackets,

$$\begin{aligned} \{r_\alpha, r_\beta\} &= 0, \\ \{p_\alpha, p_\beta\} &= 0, \\ \{r_\alpha, p_\beta\} &= \delta_{\alpha\beta}, \end{aligned} \tag{83}$$

then promote these brackets to quantum commutators. As a result, the variables become non-commutating operators and the classical theory is quantized.
An easier way to judge if the variables are canonical is by checking if they satisfy the canonical EOM,

$$\dot{\mathbf{r}} = \frac{\partial E}{\partial \mathbf{p}}; \dot{\mathbf{p}} = -\frac{\partial E}{\partial \mathbf{r}}. \tag{84}$$

The variables $\mathbf{r}_c$ and $\mathbf{k}_c$ that depict the trajectory of the wave packet are not canonical variables because their EOM are not of this form. This is due to the vector potential and the Berry connection, $\mathbf{A}(\mathbf{r}_c)$ and $\mathbf{R}(\mathbf{k}_c)$, in the Lagrangian (see Eq. (63)).
In fact, if one can remove these two gauge potentials from the Lagrangian by a change of variables,

$$L = \mathbf{p} \cdot \dot{\mathbf{r}} - E(\mathbf{r}, \mathbf{p}), \tag{85}$$

then these new variables will automatically be canonical. Such a transformation is in general non-linear and cannot be implemented easily. However, if one only requires an accuracy to linear order of the electromagnetic fields (consistent with the limit of our semiclassical theory), then the new variables can indeed be found.
The canonical variables $\mathbf{r}$ and $\mathbf{p}$ accurate to linear order in the fields are related to the center-of-mass variables as follows [35],

$$\begin{aligned} \mathbf{r}_c &= \mathbf{r} + \boldsymbol{\mathcal{R}}(\boldsymbol{\pi}) + \boldsymbol{\mathcal{G}}(\boldsymbol{\pi}), \\ \hbar\mathbf{k}_c &= \mathbf{p} + e\mathbf{A}(\mathbf{r}) + e\mathbf{B} \times \boldsymbol{\mathcal{R}}(\boldsymbol{\pi}), \end{aligned} \tag{86}$$

where $\boldsymbol{\pi} = \mathbf{p} + e\mathbf{A}(\mathbf{r})$, and $\mathcal{G}_\alpha(\boldsymbol{\pi}) \equiv (e/\hbar)(\boldsymbol{\mathcal{R}} \times \mathbf{B}) \cdot \partial\boldsymbol{\mathcal{R}}/\partial\pi_\alpha$. The last terms in both equations can be neglected in some cases. For example, they will not change the force and the velocity in Eqs. (78) and (79). These relations constitute a generalization of the Peierls substitution.
When expressed in the new variables, the semiclassical Hamiltonian in Eq. (81) becomes,

$$\begin{aligned} \mathcal{H}(\mathbf{r}, \mathbf{p}) &= \mathcal{H}_0(\boldsymbol{\pi}) - e\phi(\mathbf{r}) + e\mathbf{E} \cdot \boldsymbol{\mathcal{R}}(\boldsymbol{\pi}) \\ &+ \mathbf{B} \cdot \left[\frac{e}{2m} \boldsymbol{\mathcal{L}}(\boldsymbol{\pi}) + e\boldsymbol{\mathcal{R}} \times \frac{\partial \mathcal{H}_0}{\partial \boldsymbol{\pi}} \right], \end{aligned} \tag{87}$$

where we have used the Taylor expansion and neglected terms nonlinear in the fields. Finally, one promotes the canonical variables to quantum conjugate variables to convert $\mathcal{H}$ to an effective quantum Hamiltonian.
The dipole-energy term $e\mathbf{E} \cdot \boldsymbol{\mathcal{R}}$ is originates from the shift between the charge center $\mathbf{r}_c$ and the canonical variable $\mathbf{r}$. We will show below that for a semiconductor electron, the dipole term is in fact the spin-orbit coupling.
The correction to the Zeeman energy is also related to the Berry connection. Near a band edge, where the effective mass approximation is applicable and $E_0 = \pi^2/2m^*$, this term can be written as $e\boldsymbol{\mathcal{R}} \cdot \mathbf{v} \times \mathbf{B}$, where $\mathbf{v} = \boldsymbol{\pi}/m^*$. We know that an electron moving in a static magnetic field feels an effective electric field $\mathbf{E}_{eff} = \mathbf{v} \times \mathbf{B}$. Therefore, this term arises as a result of the electric dipole energy in electron's own reference frame.

Semiconductor electron
A necessary requirement for the non-Abelian property is that the Bloch electron has to have internal degrees of freedom. In a semiconductor with both space-inversion and time-reversal symmetries, every Bloch state is two-fold degenerate due to Kramer's degeneracy. But where do we expect to see the non-Abelian Berry connection and curvature?
Instead of the full band structure, one can start from a simpler band structure using the $\mathbf{k} \cdot \mathbf{p}$ expansion. Assuming the fundamental gap is located at $\mathbf{k} = 0$, then for small k, one has an effective Hamiltonian with 4 bands, 6 bands, 8 bands, or more, depending on the truncation. In the following discussion, we use a 8-band Kane Hamiltonian that includes the conduction band, the HH-LH bands, and the spin-orbit (SO) split-off band, each with 2-fold degeneracy (see Fig. 11). The explicit Kane Hamiltonian can be found in Ref. [36].
We focus only on the wave packet in the conduction band. Without going into details, we first show the Berry connection that is essential to the wave packet formulation. The result correct to order k^1 and up to a gauge rotation is [35],

$$\boldsymbol{\mathcal{R}} = \frac{V^2}{3} \left[\frac{1}{E_g^2} - \frac{1}{(E_g + \Delta)^2} \right] \boldsymbol{\sigma} \times \mathbf{k}, \tag{88}$$

where $V = \frac{\hbar}{m}\langle S|\hat{p}_x|X\rangle$, E_g is the energy gap, and Δ is the SO gap. Therefore, the dipole term $e\mathbf{E} \cdot \boldsymbol{\mathcal{R}}$ in Eq. (87) becomes,

$$H_{so} = e\mathbf{E} \cdot \boldsymbol{\mathcal{R}} = \alpha \mathbf{E} \cdot \boldsymbol{\sigma} \times \mathbf{k}, \tag{89}$$

where $\alpha \equiv (eV^2/3)[1/E_g^2 - 1/(E_g + \Delta)^2]$. It coincides precisely with the spin-orbit coupling of a conduction electron. This shows that the SO coupling has a very interesting connection with the Berry connection. This is also the case for the SO coupling in Dirac's relativistic electron theory [37].

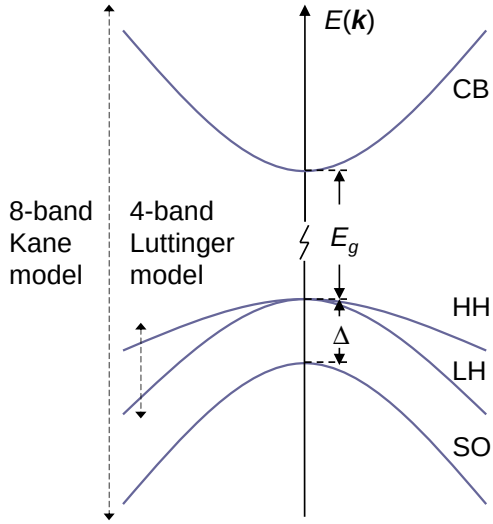

Fig. 11: *One can use the 4-band Luttinger model or the 8-band Kane model to approximate the energy bands near the fundamental gap.*

The Berry curvature calculated from Eq. (75) gives (to the lowest order) $\boldsymbol{\mathcal{F}} = \alpha/e\boldsymbol{\sigma}$, which is proportional to spin. Therefore, the anomalous velocity $e\mathbf{E} \times \mathbf{F}$ in Eq. (79) is $\alpha\mathbf{E} \times \langle\boldsymbol{\sigma}\rangle$. That is, spin-up and spin-down electrons acquire opposite transverse velocities. In non-magnetic materials, these two species have the same population and we do not expect to see a net transverse current. However, "if" one defines a spin current as the *difference* of these two transverse currents, then there will be a net *spin* current, giving rise to the spin Hall effect [38].
One can also calculate the spinning angular momentum of the conduction electron from Eq. (77). The result is,

$$\boldsymbol{\mathcal{L}} = -\frac{2mV^2}{3\hbar}\left(\frac{1}{E_g} - \frac{1}{E_g + \Delta}\right)\boldsymbol{\sigma}. \tag{90}$$

Through the Zeeman energy in Eq. (87), the orbital magnetic moment generated from Eq. (90) contributes an extra g-factor,

$$\delta g = -\frac{4}{3}\frac{mV^2}{\hbar^2}\left(\frac{1}{E_g} - \frac{1}{E_g + \Delta}\right). \tag{91}$$

This is the anomalous g-factor of the conduction electron [39]. Therefore, the anomalous g-factor in solid is indeed a result of the self-rotating motion of the electron wave packet.
Finally, the effective quantum Hamiltonian in Eq. (87) for the conduction band has the following form,

$$H(\mathbf{r}, \mathbf{p}) = E_0(\boldsymbol{\pi}) - e\phi(\mathbf{r}) + \alpha\mathbf{E} \cdot \boldsymbol{\sigma} \times \boldsymbol{\pi} + \frac{\delta g}{2}\mu_B \mathbf{B} \cdot \boldsymbol{\sigma}, \tag{92}$$

where E_0 includes the Zeeman energy from the bare spin, α is given below Eq. (89), δg is given in Eq. (91), and the correction to the Zeeman energy has been neglected. This Hamiltonian agrees with the one obtained from block diagonalization [36]. The wave packet approach is not only simpler, but also reveals the deep connections between various effective couplings and the Berry potential.
Some comments are in order: First, we emphasize again that it is necessary to include the Berry curvature and orbital moment in order to account for physical effects to first order in

external fields. Furthermore, from the discussions above, we can see that these quantities are also sufficient for building a correct quantum theory.
Second, starting from a quantum theory, one can construct a semiclassical theory in a specific subspace. This theory can later be re-quantized. The re-quantized effective theory applies to a smaller Hilbert space compared to the original quantum theory. Nevertheless, it can still have its own semiclassical theory, which in turn can again be re-quantized. As a result, a hierarchy of effective theories and gauge structures can be produced, all within the wave packet approach (see Ref. [35] for more discussions).

6 Concluding remarks

In this review, selected topics related to Berry phase in solid state physics are reported. Many of these topics have been fully developed over the years. The exposition here only serves as an introduction, without going into details and more recent development. Readers interested in certain topics can consult some of the following books or review articles: [1] and [40] on Berry phase in general, [41] and [42] on electric polarization, [43] on quantum Hall effect, [44] and [45] on anomalous Hall effect, [46] and [47] on dynamics of Bloch electrons, and [35] on non-Abelian wave packet dynamics.
In optics, the Berry curvature is related to a transverse shift (side jump) of a light beam reflected off an interface.[48] The shift is roughly the order of the wavelength. Its direction depends on the circular polarization of the incident beam. This is called the *optical Hall effect*, or the Imbert-Federov effect,[49] which is not covered here. The side jump of a light beam is similar to the analogous "jump" of an electron scattering off an impurity in the anomalous Hall effect [22]. A more detailed study of the optical transport involving spin can be found in Ref. [50].
Several topics not covered here can be found in an upcoming review on Berry phase in solid state physics [51]. These topics include the orbital magnetization of a solid, dipole moment of the wave packet, anomalous thermoelectric transport, and inhomogeneous electric polarization. It is amazing that the Berry phase plays such a versatile role in so many solid-state phenomena. On the other hand, several challenging subjects still remain largely unexplored. For example, the effect of the Berry phase in systems in which non-adiabatic processes or many-body interaction is crucial. Therefore, one can expect to see more of the intriguing Berry phase effects in solid state systems.

References

[1] A. Shapere and F. Wilczek, (ed) *Geometric Phases in Physics* (Singapore: World Scientific, 1989)

[2] For example, see p. 290 in L. I. Schiff, *Quantum Mechanics* (McGraw Hill, 3rd ed 1968)

[3] M. V. Berry, Proc. R. Soc. A **392**, 45 (1984)

[4] B. F. Schutz, *Geometrical methods of mathematical physics* (Cambridge University Press, 1980)

[5] M. Stone, Phys. Rev. D **33**, 1191 (1986)

[6] For example, see K. Ohgushi, S. Murakami, N. Nagaosa, Phys. Rev. B **62**, R6065 (2000); Y. Taguchi, Y. Oohara, H. Yoshizawa, *et al.* Science **291**, 2573 (2001); R. Shindou, N. Nagaosa, Phys. Rev. Lett. **87**, 116801 (2001)

[7] L. P. Levy *et al.* , Phys. Rev. Lett. **64**, 2074 (1990); V. Chandrasekhar *et al.* , Phys. Rev. Lett. **67**, 3578 (1991)

[8] D. Loss, P. Golbart, and A. V. Balatsky, Phys. Rev. Lett. **65**, 1655 (1990)

[9] F. Schütz, M. Kollar, and P. Kopietz, Phys. Rev. Lett. **91**, 017205 (2003)

[10] D. Loss, D. P. DiVincenzo, and G. Grinstein, Phys. Rev. Lett. **69**, 3232 (1992); J. von Delft, and C. L. Henley, Phys. Rev. Lett. **69**, 3236 (1992)

[11] See Chap 21 in R. Shankar, *Quantum Mechanics* (Springer, 2nd ed. 1994)

[12] Y. Zhang *et al.* , Nature **438**, 201 (2005).

[13] R. Resta, Ferroelectrics **136**, 51 (1992)

[14] R. D. King-Smith and D. Vanderbilt, Phys. Rev. B **47**, 1651 (1993)

[15] D. J. Thouless, Phys. Rev. B **27**, 6083 (1983); Q. Niu, Phys. Rev. Lett. **64**, 1812 (1990)

[16] K. von Klitzing, G. Dorda, and M. Pepper, Phys. Rev. Lett. **45**, 494 (1980)

[17] R. B. Laughlin, Phys. Rev. B. **23**, 5632 (1981)

[18] These mobile charges are carried through an extended state in the middle of every Landau level. Such an extended state is flanked by localized states on both sides of the energy. When the chemical potential falls within the localized states for a range of magnetic field, no charges can be transported and the Hall conductance exhibits a plateau over this range of magnetic field. Without disorder, there will be no localized states, thus no plateaus. Therefore, disorder also plays a crucial role in the quantum Hall effect.

[19] J. D. Thouless, M. Kohmoto, P. Nightingale, and M. den Nijs, Phys. Rev. Lett. **49**, 405 (1982); Also see M. Kohmoto Ann. Phys. (N.Y.) **160**, 355 (1985)

[20] Because the vector potential $\mathbf{A}_0$ in the unperturbed Hamiltonian H_0 breaks the lattice symmetry, one needs to solve the Schrödinger equation based on the so-called magnetic translation symmetry. Therefore, to be precise, the Bloch state, the Bloch energy, and the Brillouin zone mentioned here for the QHE should actually be the magnetic Bloch state, the magnetic Bloch energy, and the magnetic Brillouin zone, respectively. This distinction is not emphasized in the text.

[21] Q. Niu, D. J. Thouless, and Y. S. Wu, Phys. Rev. B **31**, 3372 (1985)

[22] L. Berger and G. Bergmann, in *The Hall Effect and Its Applications* edited by C. L. Chien, and C. R. Westgate (Plenum, New York, 1979) p. 55.

[23] Another often mentioned explanation is the side-jump mechanism proposed by Berger in 1970. It involves the impurity scattering but the underlying formalism can be rephrased in a way related to the Berry connection. It also predicts $\rho_H \propto \rho_L^2$. One can consult Ref. [22] for more details.

[24] R. Karplus and J. M. Luttinger, Phys. Rev. **95**, 1154 (1954)

[25] J. Smit, Physica **21**, 877 (1955)

[26] Y. Taguchi, Y. Oohara, H. Yoshizawa, N. Nagaosa, and Y. Tokura, Science **291**, 2573 (2001); T. Jungwirth, Q. Niu, and A. H. MacDonald, Phys. Rev. Lett. **88**, 207208 (2002)

[27] Z. Fang *et al.* , Science **302**, 92 (2003)

[28] C. Zeng, Y. Yao, Q. Niu, and H. Weitering, Phys. Rev. Lett. **96**, 37204 (2006)

[29] M. C. Chang, and Q. Niu, Phys. Rev. B **53**, 7010 (1996); G. Sundaram and Q. Niu, Phys. Rev. B **59**, 14915 (1999)

[30] D. Xiao, Y. Yao, Z. Fang, and Q. Niu, Phys. Rev. Lett. **97**, 026603 (2006).

[31] P. C. Chuu, M. Chang, and Q. Niu to be published

[32] S. E. Novoselov *et al.* , Nature **438**, 197 (2005); Y. Zhang *et al.* , Nature **438**, 201 (2005)

[33] D. Culcer, Y. Yao, and Q. Niu, Phys. Rev. B **72**, 85110 (2005)

[34] F. Wilczek, and A. Zee, Phys. Rev. Lett. **52**, 2111 (1984)

[35] M. C. Chang, and Q. Niu, J. Phys.: Condens. Matter **20**, 193202 (2008)

[36] R. Winkler *Spin-orbit coupling effects in two-dimensional electron and hole systems* (Springer, 2003)

[37] H. Mathur, Phys. Rev. Lett. **67**, 3325 (1991); R. Shankar, and Mathur, Phys. Rev. Lett. **73**, 1565 (1994)

[38] S. Murakami, N. Nagaosa, and S. C. Zhang, Science **301**, 1348 (2003)

[39] See Problem 9.16 in P. Y. Yu and M. Cardona *Fundamentals of Semiconductors* the third ed. (Springer, 2003)

[40] A. Bohm, A. Mostafazadeh, H. Koizumi, Q. Niu, and J. Zwanziger, *The Geometric Phase in Quantum Systems* (Springer-Verlag, Heidelberg, 2003)

[41] R. Resta, Rev. Mod. Phys. **66**, 899 (1994)

[42] R. Resta, J. Phys.: Condens. Matter **12**, R107 (2000)

[43] R. E. Prange, and S. M. Girvin, *The quantum Hall effect* (Springer, 2nd ed., 1990)

[44] N. Nagaosa, J. Phys. Soc. Jpn. **75**, 042001 (2006)

[45] N. A. Sinitsyn, J. Phys: Condens. Matter **20**, 023201 (2008)

[46] E. I. Blount, *Solid State Physics*, edited by Seitz F and Turnbull D (Academic Press Inc., New York, 1962), Vol. 13

[47] G. Nenciu, Rev. Mod. Phys. **63**, 91 (1991)

[48] M. Onoda, S. Murakami, and N. Nagaosa, Phys. Rev. Lett. **93**, 83901 (2004); K. Sawada, and N. Nagaosa, Phys. Rev. Lett. **95**, 237402 (2005); M. Onoda, S. Murakami, and N. Nagaosa, Phys. Rev. E **74**, 66610 (2006)

[49] F. I. Fedorov, Dokl. Akad. Nauk SSSR **105**, 465 (1955); C. Imbert, Phys. Rev. D **5**, 787 (1972);

[50] K. Y. Bliokh *et al.*, Phys. Rev. Lett. **96**, 073903 (2006); K. Bliokh, Phys. Rev. Lett. **97** 043901 (2006); C. Duval et al., Phys. Rev. D **74**, 021701 (R) (2006)

[51] D. Xiao, M. C. Chang, and Q. Niu, to be published